Structures and Buildings
Volume 165 Issue SB10

Strain gradient effects on concrete stress–strain curve
Peng and Ho

ice | proceedings

Proceedings of the Institution of Civil Engineers
Structures and Buildings 165 November 2012 Issue SB10
Pages 543–565 http://dx.doi.org/10.1680/stbu.10.00056
Paper 1000056
Received 19/10/2010 Accepted 10/10/2011
Published online 22/02/2012
Keywords: columns/concrete structures/design methods & aids

ice
Institution of Civil Engineers
publishing

Strain gradient effects on concrete stress–strain curve

1 **Jun Peng** MPhil
PhD Student, Department of Civil Engineering, University of Hong Kong, Hong Kong

2 **Johnny Ching Ming Ho** PhD, MHKIE, MIEAust, CPEng
Assistant Professor, Department of Civil Engineering, University of Hong Kong, Hong Kong

The stress–strain characteristic of concrete developed in flexure is one of the essential parameters for the ultimate flexural strength design of reinforced concrete (RC) members. Currently, the stress–strain curve of concrete developed in flexure is obtained by scaling down the uniaxial stress–strain curve. In current RC design codes, it is represented by an equivalent rectangular concrete stress block depending solely on the concrete strength. By comparing the theoretical strength evaluated for the stress block with the measured strength, the authors found that current codes underestimate the actual flexural strength of RC beams and columns by 9% and 19%, respectively. Since the underestimation is different for beams and columns, which are subjected to different strain gradients at ultimate, it is suggested that the maximum concrete stresses developed in flexure should depend also on strain gradient. The effects of strain gradient on the concrete stress developed in flexure were investigated in this work by testing RC columns under concentric and eccentric axial loads or horizontal loads. The concrete stress–strain curves of the eccentrically/horizontally loaded specimens were derived by modifying those of concentrically loaded counterparts based on axial force and moment equilibriums. The results indicate that the maximum concrete stress developed in flexure depends significantly on strain gradient. Formulas were developed to correlate the maximum and equivalent concrete stresses developed in flexure to the strain gradient. Their applicability was verified by comparing the results with measured flexural strengths of RC beams and columns.

Notation

A_c area of concrete compression zone
A_g column cross-section area
A_s area of steel bar
b width of cross-section
c neutral axis depth
d effective depth of column section
d_i distance of longitudinal steel bar to extreme compressive fibre or effective depth of cross-section in Equations 3, 4 and 5
E_s Young's modulus of steel bar
f_{av} average concrete compressive stress over compression area in flexural members
f'_c uniaxial concrete compressive strength represented by cylinder strength
f_{cu} uniaxial concrete compressive strength represented by cube strength
f_{max} maximum concrete compressive stress developed under flexure
f_s stress of steel bar in Equations 3, 4 and 5
f_y yield strength of steel bar
h height of cross-section
k_1 ratio of average stress (f_{av}) over compression area to maximum stress developed under flexure (f_{max})
k_2 ratio of distance between extreme compressive fibre and resultant force of compressive stress block ($\boldsymbol{P}_c$) to that between the same fibre to the neutral axis (c)
k_3 ratio of f_{max} to concrete cube strength f_{cu}
k'_3 ratio of f_{max} to the maximum uniaxial concrete strength σ_{max}
$\boldsymbol{M}$ moment or flexural strength
$\boldsymbol{M}_{ACI}$ moment calculated based on ACI 318 (ACI, 2008)
$\boldsymbol{M}_{EC}$ moment calculated based on Eurocode 2 (CEN, 2004)
$\boldsymbol{M}_{NZ}$ moment calculated based on NZS 3101 (SNZ, 2006)
$\boldsymbol{M}_p$ moment calculated based on the proposed values of equivalent rectangular concrete stress block parameters obtained in this study
$\boldsymbol{M}_t$ measured moment capacity
n number of longitudinal steel bars
$\boldsymbol{P}$ axial load

$\boldsymbol{P}_c$	resultant force of concrete compressive stress block
α	ratio of equivalent concrete compressive stress developed under flexure to concrete cube strength (f_{cu})
β	ratio of height of equivalent rectangular concrete compressive stress block to neutral axis depth
ε	concrete strain
ε_{cu}	ultimate concrete strain at extreme compressive fibre measured at maximum load of eccentrically or horizontally loaded specimen
ρ_s	longitudinal reinforcement ratio
σ	concrete stress
σ_{max}	maximum concrete compressive stress developed in concentrically loaded specimen
ϕ	strain gradient

1. Introduction

In the current reinforced concrete (RC) design codes, the concrete stress distribution within the compression zone of a typical RC section subjected to bending at ultimate state is non-linear, as shown in Figure 1. This stress–strain curve of concrete is derived by scaling down the stress–strain curve of concrete developed in uniaxial compression to 67% of the compressive strength of standard concrete cubes. This factor, which was derived from converting 85% of standard concrete cylinder strength to the respective cube strength proposed by Hognestad *et al.* (1955), is to account for the different concrete strengths developed in standard concrete cubes, f_{cu}, and real columns. In ultimate flexural strength design of RC sections, the non-linear concrete stress distribution is represented by a concrete stress block defined by three parameters, k_1, k_2 and k_3 (Hognestad *et al.*, 1955; Ibrahim and MacGregor, 1996, 1997; Kaar *et al.*, 1978; Tan and Nguyen, 2004, 2005). k_1 is the ratio of average stress, f_{av}, over the compression zone to maximum stress developed under flexure, f_{max}, k_2 is the ratio of distance between the extreme compressive fibre and the resultant force of the stress block ($\boldsymbol{P}_c$) to that between the same fibre to the neutral axis (c) and k_3 is the ratio of f_{max} to uniaxial concrete cube (or cylinder) strength. This stress block was further simplified to an equivalent rectangular concrete stress block (Hognestad, 1957; Kriz, 1959; Mattock *et al.*, 1961; Whitney, 1940) to facilitate practical flexural strength design of RC members, which are currently being adopted in RC design codes such as Eurocode 2 (CEN, 2004), NZS 3101 (SNZ, 2006) and ACI 318 (ACI, 2008).

The equivalent rectangular concrete stress block (Figure 1(e)) is defined by two parameters, α and β: α is the ratio of the equivalent concrete compressive stress developed under flexure to the concrete cube strength, f_{cu}; β is the ratio of the height of the equivalent rectangular concrete stress block to the neutral axis depth (c). An ideal equivalent rectangular concrete stress block could give an exact representation of the magnitude and location of the resultant concrete compressive force and thus the flexural strength of RC members. The values of α and β currently adopted by various RC design codes (ACI, 2008; CEN, 2004; SNZ, 2006), which are dependent only on the concrete strength, are summarised in Table 1. The accuracy of these equivalent stress blocks in predicting the flexural strength of RC members can be studied by comparing the theoretical with the measured flexural strengths of RC beams and columns tested by other researchers. The comparison is shown in Table 2. From the table, it is evident that the equivalent rectangular concrete stress block can predict fairly accurately the strength of columns subjected to very high axial load levels, but underestimates the flexural strength of other columns and beams. The underestimation of strength is about 9% for beams and 19% for columns subjected to low to medium axial load levels. These phenomena should be dealt with cautiously because this will underestimate the shear demands of beams and columns in moment-resisting frame buildings, which will lead to premature shear failure (Arslan, 2010; Baczkowski and Kuang, 2008; Bukhari *et al.*, 2010; Lu *et al.*, 2009; Pam and Ho, 2001). The underestimation of maximum concrete strength developed in flexure will also overestimate the available ductility and rotational capacity of the lowest storey columns of a moment-resisting frame building (Arslan *et al.*, 2010; Do Carmo and Lopes, 2006; Ho and Pam, 2010; Inel *et al.*, 2007; Sebastian and Zhang, 2008; Shim *et al.*, 2008; Wu *et al.*, 2004). Then, plastic hinges cannot be formed (Bai and Au, 2008; Jaafar, 2008; Pam and Ho, 2009) and the desirable 'beam sidesway mechan-

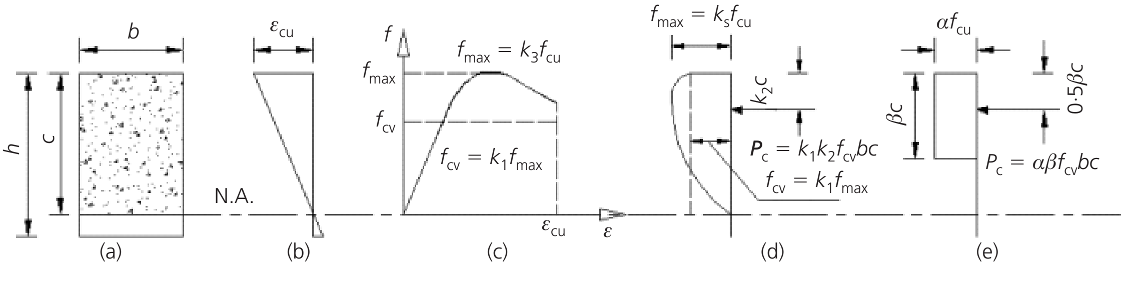

Figure 1. Concrete stress block parameters. (a) Cross-section. (b) Strain distribution at ultimate state. (c) Stress–strain curve under flexure. (d) Actual stress distribution at ultimate state. (e) Equivalent rectangular stress block

Design code	α	β
ACI 318 (ACI, 2008)	0·85 for all f'_c	0·85 for $f'_c \leqslant 28$ MPa $0{\cdot}85 - 0{\cdot}007(f'_c - 28) \geqslant 0{\cdot}65$ for $f'_c > 28$ MPa
Eurocode 2 (CEN, 2004)	0·85 for $f'_c \leqslant 50$ MPa $0{\cdot}85 - 0{\cdot}85\left(\dfrac{f'_c - 50}{200}\right)$ for $50 < f'_c \leqslant 90$MPa	0·80 for $f'_c \leqslant 50$ MPa $0{\cdot}8 - \left(\dfrac{f'_c - 50}{400}\right)$ for $50 < f'_c \leqslant 90$ MPa
NZS 3101 (SNZ, 2006)	0·85 for $0 < f'_c \leqslant 55$ MPa $0{\cdot}85 - 0{\cdot}004(f'_c - 55)$ for $55 < f'_c \leqslant 80$ MPa 0·75 for $f'_c > 80$ MPa	0·85 for $0 < f'_c \leqslant 30$ MPa $0{\cdot}85 - 0{\cdot}008(f'_c - 30)$ for $30 < f'_c \leqslant 55$ MPa 0·65 for $f'_c > 55$ MPa

Table 1. The values of equivalent concrete stress block parameters stipulated in RC design codes

ism' cannot be developed to allow moment redistribution (Oehlers *et al.*, 2010; Spence, 2008; Zhou and Zheng, 2010) to occur during extreme events such as earthquake attack and accidental impact (Chen and May, 2009; Inel *et al.*, 2008; Jones and Fraser, 2009) The consequence is that the columns would fail in a brittle manner without ample warning. For gravity-load-resisting structures, the overestimation of flexural strength will unnecessarily increase the member size and carbon content of the buildings, which reduces energy efficiency. Although the design of flexural ductility may be considered less important in a gravity-load-resisting structure, underestimation of flexural ductility will reduce the level of structural safety when it is subjected to extreme loads such as overloading, blasting and sudden impact.

From the comparison shown in Table 2, it is apparent that underestimation of flexural strength by the equivalent rectangular stress block of various design codes is different in beams and columns. Since the strain gradient in beams and columns is different at the ultimate state due to the presence of axial load, it is believed that the underestimation may be attributed to the effects of strain gradient. In fact, some researchers investigated the effects of strain gradient on the concrete stress–strain curve developed in flexure many years ago. Sturman *et al.* (1965) determined the stress–strain curve of normal-strength concrete (NSC) developed under concentric and eccentric loads and found that the maximum concrete stress that can be developed in eccentrically loaded columns was higher than that in concentrically loaded columns. Clark *et al.* (1967) reported that the maximum stress developed in NSC increases as strain gradient increases. Soliman and Yu (1967) derived the NSC stress–strain curve in flexure and pointed out that the maximum stress increased as the volume of transverse steel increased (i.e. as strain gradient increased). Smith and Orangun (1969) derived a fourth-order polynomial for the concrete stress–strain developed in flexure, which was significantly different from that of the uniaxial concrete compression curve. More recently, Tan and Nguyen (2004) derived stress–strain curves for NSC and high-strength concrete (HSC) (up to 76 MPa) in flexure based on experimental results and found that the maximum concrete stress developed in flexure is higher than that in uniaxial compression. This also agreed with the test results obtained by Yi *et al.* (2002) who reported that the maximum and equivalent concrete stresses decrease as column size increases (i.e. as strain gradient decreases). Tabsh (2006) also reported on the strain gradient effect in the HSC stress–strain curve developed under flexure.

In this work, the effects of strain gradient on the maximum concrete stress and equivalent rectangular concrete stress block developed in flexure were studied experimentally by testing 16 inverted T-shaped column specimens under concentric and eccentric axial loads, as well as horizontal load. The specimens were divided into six groups, each of which contained specimens with identical cross-section properties. In each group, one specimen was subjected to concentric load while the rest was/were subjected to eccentric or horizontal loads. To study the effects of strain gradient, the ratio of the maximum concrete compressive stress developed in the specimens subjected to eccentric/horizontal load to the maximum uniaxial compressive stress (σ_{max}) developed in the counterpart specimens subjected to concentric load (denoted by k'_3) was determined based on axial force and moment equilibriums. Using the obtained value of k'_3, the stress block parameters k_1, k_2 and k_3 and the equivalent concrete stress block parameters α and β were determined. From the test results, it was found that the currently adopted values of k_3 and α are only applicable to RC members subjected to a small strain gradient. For a larger strain gradient, these parameters increased as strain gradient increased. On the other hand, k_1, k_2 and β remained relatively constant irrespective of strain gradient. To facilitate practical flexural strength design of RC members, formulas correlating k_3, α and β to the strain gradient are proposed. The applicability of these formulas is verified by comparing the theoretical flexural strength evaluated using the proposed formula with the measured strength of RC beams and columns obtained by other researchers. Lastly, the effects of strain gradient on the

Specimen code	f'_c: MPa	$P/A_g f'_c$	Moment: kNm				$\frac{(1)}{(4)}$	$\frac{(2)}{(4)}$	$\frac{(3)}{(4)}$
			M_{ACI} (1)	M_{EC} (2)	M_{NZ} (3)	M_t (4)			
Beams									
A[a]	41·3	—	97·0	97·0	97·0	104·0	0·93	0·93	0·93
B[a]	41·3	—	45·0	45·0	45·0	49·6	0·91	0·91	0·91
T3[b]	27·7	—	28·9	29·3	28·9	32·5	0·89	0·90	0·89
T6[b]	27·7	—	170·5	171·2	170·5	192·4	0·89	0·89	0·89
Columns subjected to low axial load level									
C1-1[c]	24·9	0·113	300·5	305·1	300·5	351·4	0·86	0·87	0·86
C1-2[c]	26·7	0·106	303·8	308·2	303·8	374·6	0·81	0·82	0·81
C2-2[c]	27·1	0·156	325·2	330·5	325·2	399·9	0·81	0·83	0·81
Columns subjected to medium axial load level									
C3-3[c]	26·9	0·209	335·4	345·9	335·4	423·8	0·79	0·82	0·79
X6[d]	31·9	0·450	28·5	29·0	28·6	37·1	0·77	0·78	0·77
X7[d]	35·7	0·450	29·7	30·5	29·8	37·1	0·80	0·82	0·80
SBCM-8[e]	28·0	0·220	46·0	46·0	46·0	58·7	0·78	0·78	0·78
Columns subjected to high axial load level									
A-16[f]	33·9	0·600	157·1	159·1	157·6	157·5	1·00	1·01	1·00
E-2[f]	31·4	0·610	160·1	163·5	160·5	169·3	0·95	0·97	0·95
Columns subjected to ultra-high axial load level									
E-8[f]	25·9	0·780	128·4	129·2	128·4	129·2	0·99	1·00	0·99
E-10[f]	26·3	0·770	130·6	131·3	130·6	132·7	0·98	0·99	0·98

[a]Pecce and Fabbrocino (1999)
[b]Debernardi and Taliano (2002)
[c]Mo and Wang (2000)
[d]Lam *et al.* (2003)
[e]Marefat *et al.* (2005)
[f]Sheikh and Yeh (1990)

Table 2. Comparison of flexural strengths obtained from codes and previous tests

maximum concrete stress developed in flexure will be explained using the previous test observations on the progressive development of concrete micro-cracking in pure axially loaded and flexural NSC columns obtained by Sturman *et al.* (1965).

2. Test programme

2.1 Experimental setup and details of specimens

Sixteen inverted T-shaped square column specimens with concrete cube strength ranging from 32 to 58 MPa were fabricated and tested under concentric and eccentric axial loads or horizontal loads. They were divided into six groups, with each group comprising specimens with identical cross-section and material strength properties. Concrete for the same group of specimens was cast from the same batch of concrete transported by the same truck from the same plant. They were also cured under the same environmental conditions and thus the concrete strength for all specimens within the same group can be regarded as identical. One of the specimens in each group was tested under concentric load, while the rest were tested under eccentric axial load (for small strain gradient) or horizontal load (for large strain gradient). The specimens had a cross-section of $400 \times 400\ \mathrm{mm}^2$. The height of the columns was 1400 mm and the length of the supporting beams 1500 mm, as shown in Figure 2. For specimens

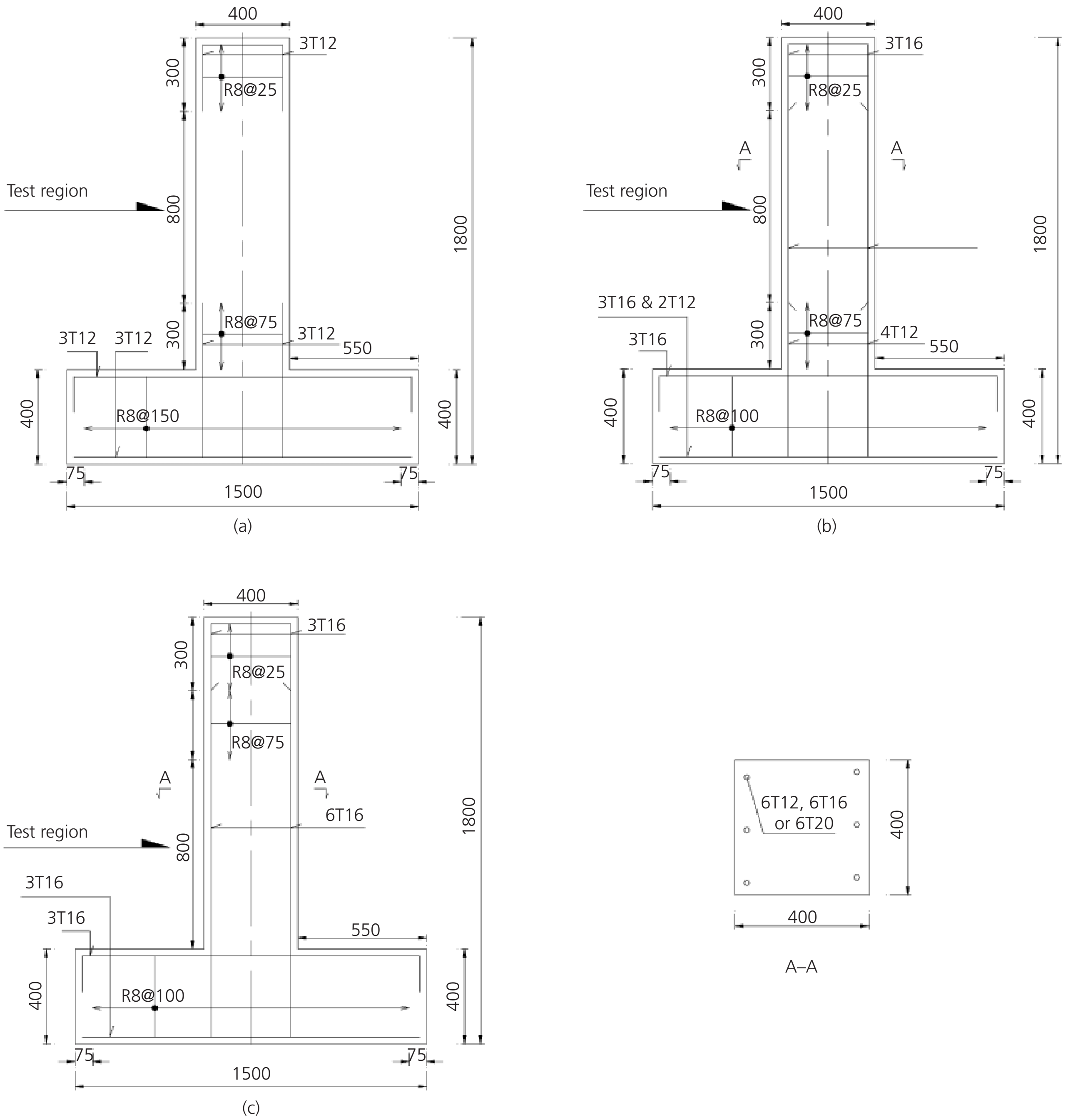

Figure 2. (a) PC specimen. (b) Eccentrically loaded RC specimen. (c) Horizontally loaded RC specimen. Dimensions in mm

tested under concentric and eccentric axial loads, the testing regions were in the middle 800 mm of the column height. For specimens tested under horizontal load, the testing regions were within 800 mm from the beam–column interface. Outside the testing regions, the columns were heavily confined with transverse steel and/or square hollow steel tube (400×400 mm^2) so that failure would always take place in the pre-determined testing regions. The plain concrete (PC) specimens did not contain any longitudinal steel within the testing region, while RC specimens contained different amounts of longitudinal steel with steel ratios of 0·42–1·18%. The cross-section properties and material strengths of each test specimen are listed in Table 3; the values are those commonly adopted by other researchers (Ahn and Shin, 2007; Choi *et al.*, 2009; Han *et al.*, 2010; Kim *et al.*, 2007; Sim *et al.*, 2009; Supaviriyakit *et al.*, 2007; Xiao *et al.*, 2008). The specimens were coded as follows. The first number refers to the concrete cube strength on day 28 and the second number refers to the percentage longitudinal steel ratio.

The uniaxial concrete stress–strain behaviour in each group of specimens was obtained by testing one of the specimens under concentric axial load. For RC specimens, the concrete stress was obtained by subtracting the steel force from the total applied load and then the difference was divided by the concrete area. The strain was obtained by dividing axial shortening of the specimen (measured with linear variable displacement transducer (LVDTs)) by its gauge length. The concrete stress–strain curve developed in flexure (with strain gradient) was obtained by modifying the obtained uniaxial concrete stress–strain curve such that the theoretical axial force and moment matched the experimentally measured values. For the specimens tested under eccentric loading, different eccentricities (ranging from 50 to 140 mm as summarised in Table 3) were used to simulate different extents of strain gradient in columns at ultimate state. Nevertheless, since the maximum eccentricity, which is restricted by the column size, was about 150 mm, specimens that needed to be tested under larger eccentricities to simulate the effects of large strain gradient were tested under simultaneous axial and horizontal loads.

The test setup for the three types of loading is shown in Figure 3. The axial and horizontal loads applied to the columns were produced by a computerised electro-hydraulic servo controlled multi-purpose testing machine having a maximum loading capacities of 10 000 and 1500 kN, respectively.

Because of the different loading arrangements, the failure modes of the specimens were different. When a column was subjected to concentric load or small eccentricity, it would fail in compression where the tension steel would not yield. However, when a column was subjected to large eccentricity or simultaneous axial and horizontal loads, it would fail in tension where the tension steel would yield. These failure modes are represented by different locations on the interaction curve of the column specimens (Figure 4).

2.2 Instrumentation

Instrumentation to monitor the behaviour of the column specimens included strain gauges and LVDTs (Figure 5)

Group	Specimen code	Loading mode	Longitudinal steel				f_{cu}: MPa		Eccentricity: mm
			ρ_s: %	Detail	f_y: MPa	E_s: GPa	Day 28	Testing day	
1	PC35-0-CON	Concentric	0	—	—	—	35·0	35·0	0
	PC35-0-ECC	Eccentric	0	—	—	—		35·3	120
2	RC30-0·42-CON	Concentric	0·42	6T12	538	203	30·0	35·9	0
	RC30-0·42-ECC	Eccentric						35·9	140
3	RC28-0·75-CON	Concentric	0·75	6T16	533	203	28·2	33·6	0
	RC28-0·75-ECC	Eccentric						31·6	140
4	RC38-1·18-CON	Concentric	1·18	6T20	536	200	38·4	43·2	0
	RC38-1·18-ECC	Eccentric						42·8	110
5	RC50-0·75-CON	Concentric	0·75	6T16	515	203	50·3	50·3	0
	RC50-0·75-ECC-1	Eccentric						58·2	120
	RC50-0·75-ECC-2	Eccentric						58·2	140
6	RC41-0·75-CON	Concentric	0·75	6T16	498	198	40·6	42·1	0
	RC41-0·75-ECC-1	Eccentric						49·1	50
	RC41-0·75-ECC-2	Eccentric						49·1	130
	RC41-0·75-HOR-1	Horizontal						46·4	—
	RC41-0·75-HOR-2	Horizontal						46·4	—

Table 3. Specimen properties

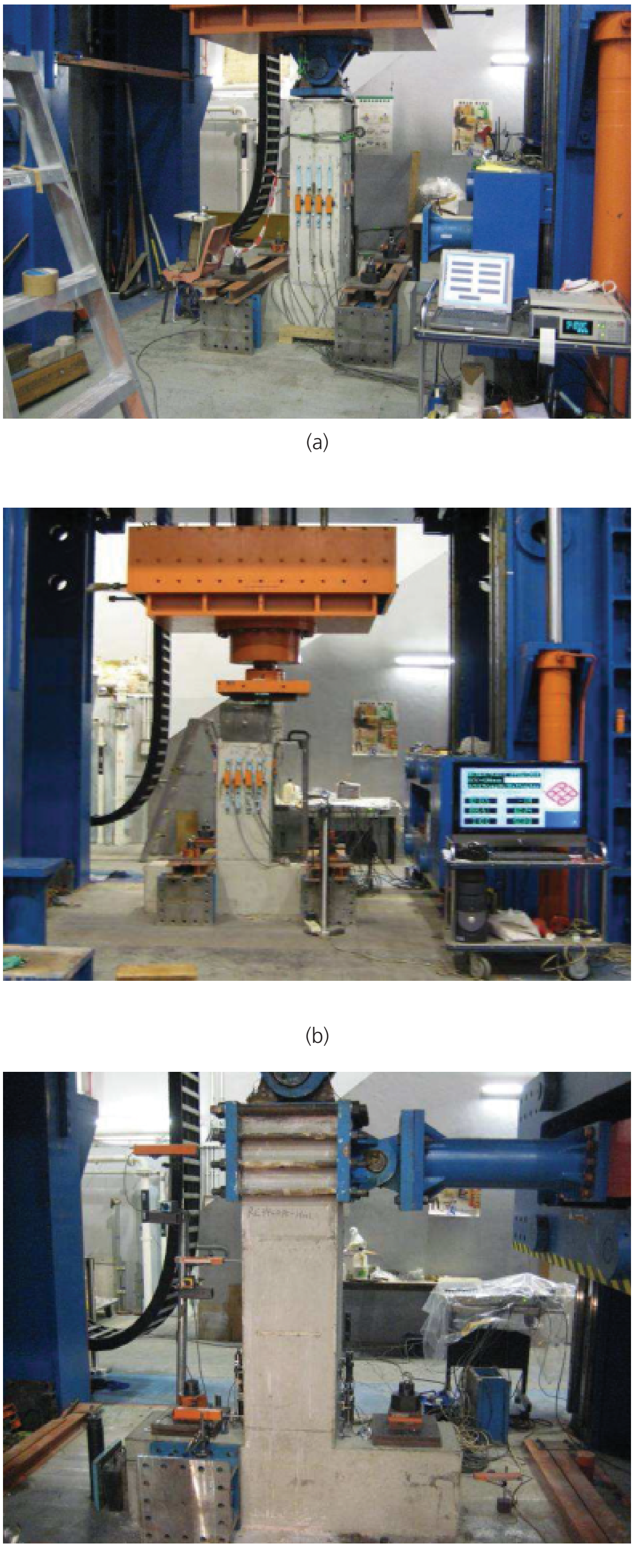

(a)

(b)

(c)

Figure 3. Loading setup: (a) concentric loading; (b) eccentric loading; (c) horizontal and axial loading

(*a*) Strain gauges were adopted for both steel and concrete. The steel strain gauges were attached to the longitudinal steel bars located within the testing region. The concrete strain gauge(s) was/were attached on each face of every concentric and eccentric specimen. For the horizontally loaded specimens, concrete strain gauges were attached on the extreme tension and compression column faces.

(*b*) For specimens subjected to concentric and eccentric loads, a total of 12 LVDTs were installed on four sides of the specimen within the test area to measure the deformation due to axial load and/or bending moment. For specimens subjected to horizontal load, three LVDTs were installed on each of the extreme tension and compression column faces.

2.3 Testing procedure

For specimens subjected to concentric and eccentric loads, vertical load application was set in a displacement-controlled manner at a rate of 0·36 mm/min. For horizontally loaded specimens, the prescribed axial load was applied first. Horizontal load was then applied in a displacement-controlled manner at a rate of 0·5 mm/min. Load application was stopped after the applied load had reached the maximum value and then dropped below 80% of the maximum value.

3. Experimental results

3.1 Concentric specimens

Example of specimens tested under concentric, eccentric and horizontal loads after failure are shown in Figures 6(a), 6(b) and 6(c) respectively. The measured concrete compressive forces of the concentrically loaded column specimens are plotted against their corresponding axial displacements in Figure 7. The total concrete compressive force is taken as the total compressive axial load applied by the actuator for PC specimens, while that of RC specimens was obtained by subtracting the compressive forces in longitudinal steels from the applied axial loads. All steel reinforcements adopted in the test were hot-rolled high-yield deformed bars of characteristic yield strength of not less than 460 MPa. For this type of steel, it has been commonly accepted for decades that a linearly elastic–perfectly plastic stress–strain curve can be used to describe the uniaxial stress–strain behaviour. The same stress–strain curve will be adopted for the steel reinforcement used in this study to determine the steel stress from the corresponding strain measured in the test by the strain gauges. The concrete stress–strain curves for all concentrically loaded specimens are also shown in Figure 7; these will be used to determine the maximum concrete compressive stress that can be developed in the counterpart eccentrically/horizontally loaded specimens. The strains of concrete were obtained by dividing the LVDT readings with the gauge length; they show good agreement with the strains measured by the concrete strain gauges (Figure 8). From Figure 7, it is evident that the concrete compressive force–displacement and stress–strain curves are fairly linear up to about 50% of the maximum force (stress). After this, the displacement (strain) increases more rapidly than the concrete

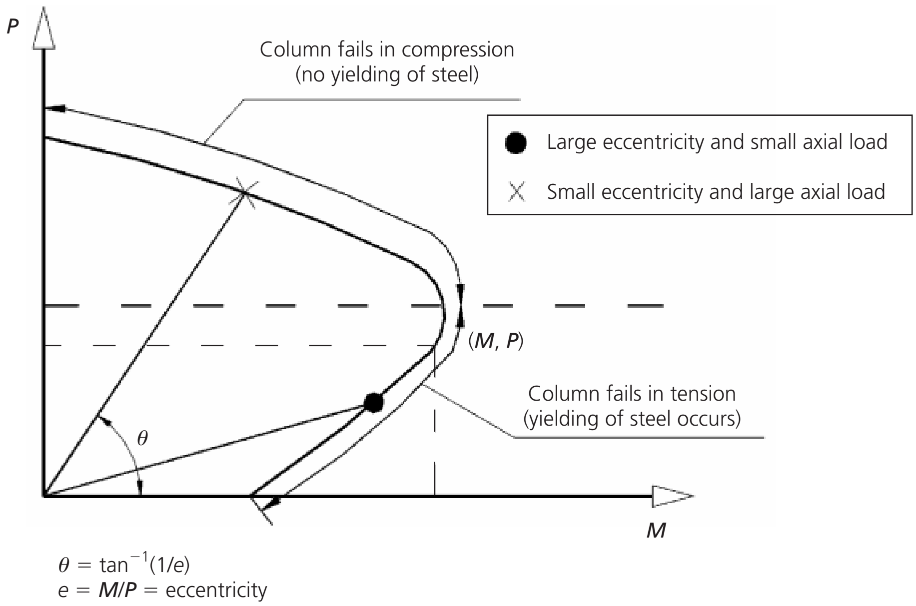

Figure 4. Failure modes and column interaction

compressive force (stress) due to the rapid degradation of column stiffness.

3.2 Eccentric/horizontal specimens

The measured concrete compressive forces of the eccentrically loaded specimens are plotted against actuator-measured vertical displacements of the column in Figure 9(a). Similarly, the concrete compressive forces of the RC specimens were obtained by subtracting the steel forces from the respective total applied loads. For the specimens tested under horizontal load, the measured horizontal load is plotted against its lateral drift in Figure 9(b). The maximum moment acting on the eccentrically loaded specimens was evaluated by multiplying the applied axial load by the eccentricity; for horizontally loaded specimens, the moment was obtained by multiplying the horizontal load by the lever arm (i.e. the vertical distance from the horizontal actuator to the beam–column interface). With the obtained maximum axial loads and moments, the concrete stress distribution developed in the eccentrically and horizontally loaded specimens with strain gradient effect can be investigated.

4. Derivation of concrete stress block parameters

4.1 Derivation of stress block parameters k_1, k_2 and k_3

The ratio of the maximum concrete stress developed in flexure to the concrete cube strength, k_3, will be determined by equating the theoretical axial force and moment with the measured values of the eccentrically or horizontally loaded specimens. The theoretical values can be computed based on the stress–strain curve obtained from the concentrically loaded specimens multiplied by k_3', which is defined as the ratio of the maximum concrete stress developed in eccentrically or horizontally loaded specimens to its uniaxial strength in concentrically loaded columns, to take into account the effects of strain gradient. Firstly, the uniaxial concrete stress–strain curve of each concentrically loaded specimen was obtained by fitting the measured stress and strain data using the parabolic function

$$1.\quad \sigma = A\varepsilon^2 + B\varepsilon$$

where σ and ε are the concrete stress and strain developed in concentrically loaded specimens, respectively, and A and B are coefficients obtained from regression analysis. From the definition of k_3', the concrete stress–strain curve developed in eccentrically or horizontally loaded specimens with strain gradient effect can be obtained by multiplying both sides of Equation 1 by k_3'

$$2.\quad k_3'\sigma = k_3'(A\varepsilon^2 + B\varepsilon)$$

where $k_3'\sigma$ is the concrete stress developed in flexure. The value of k_3' and c for each eccentrically or horizontally loaded specimen can be determined by considering the axial force (***P***) and moment (***M***) equilibriums of the eccentrically or horizontally loaded column section, as expressed by Equations 3a and 3b, respectively (compression is taken as positive). Finally, the value of k_3 can be determined using Equation 3d.

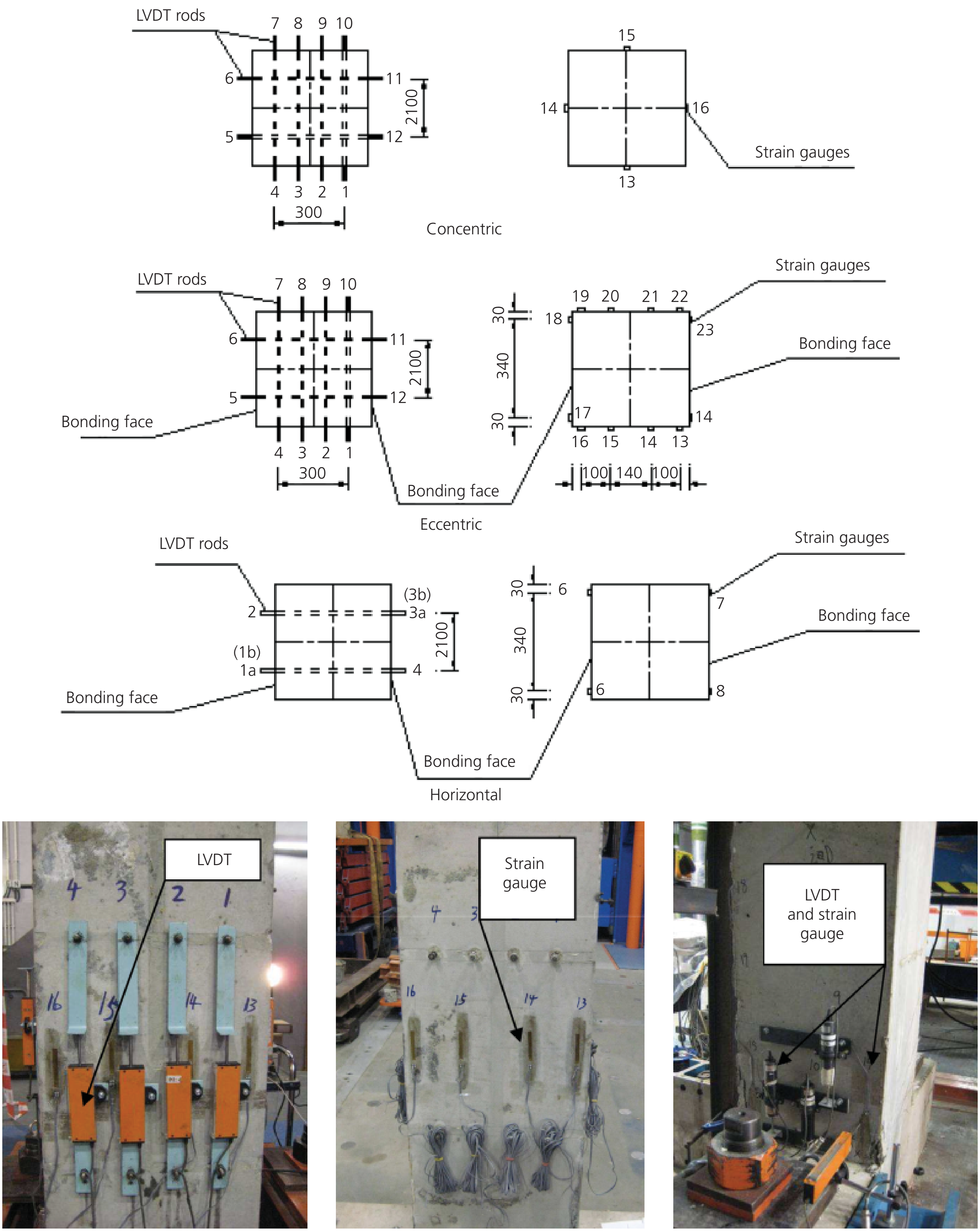

LVDT (eccentric)

Strain gauge (eccentric)

LVDT & strain gauge (horizontal)

Figure 5. Specimen instrumentation

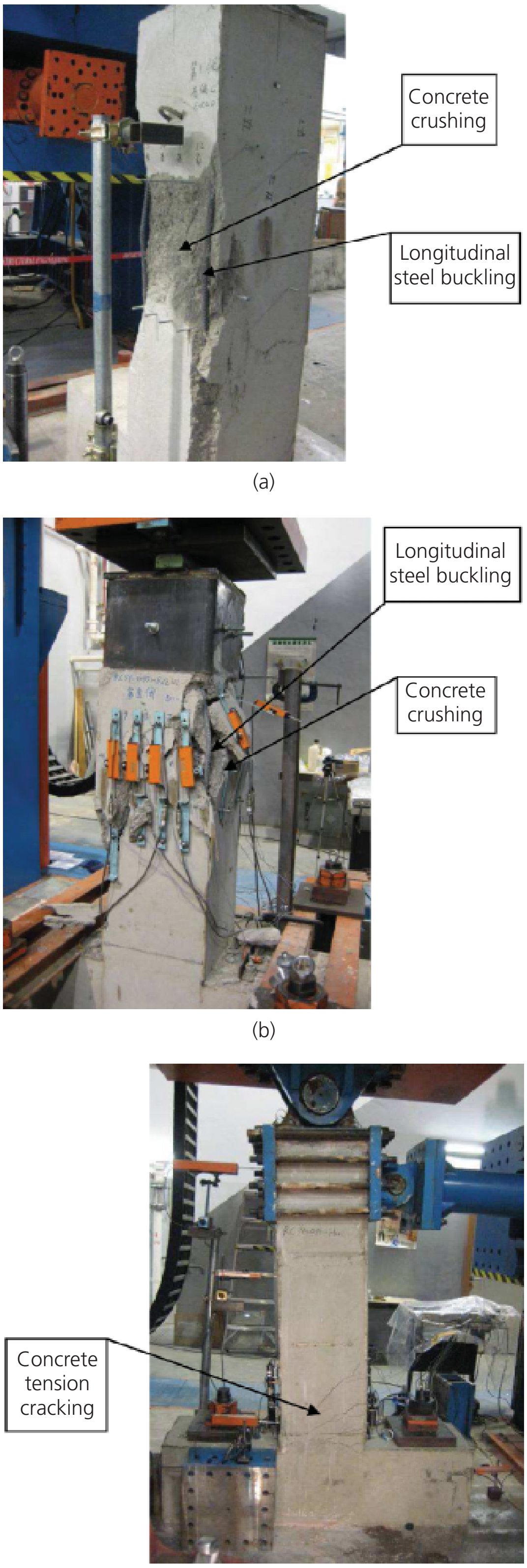

Figure 6. Selected specimens after failure: (a) RC41-0·75-CON; (b) RC41-0·75-ECC-1; (c) RC41-0·75-HOR-1

$$\boldsymbol{P} = \int_{A_c} k_3(A\varepsilon^2 + B\varepsilon)\,\mathrm{d}A_c + \sum_{i=1}^{n} f_{si}A_{si} \quad \text{3a.}$$

$$\boldsymbol{M} = \int_{A_c} k_3(A\varepsilon^2 + B\varepsilon)\left(\frac{h}{2} - c + x\right)\mathrm{d}A_c + \sum_{i=1}^{n} f_{si}A_{si}\left(\frac{h}{2} - d_i\right) \quad \text{3b.}$$

$$\varepsilon = (x/c)\varepsilon_{cu} \quad \text{3c.}$$

$$k_3 = k_3'(\sigma_{max}/f_{cu}) \quad \text{3d.}$$

where A_c is the area of concrete compression zone, x is the distance of strip $\mathrm{d}A_c$ from the neutral axis, n is the total number of steel bars, f_{si} and A_{si} are, respectively, the stress and area of the ith steel bar, d_i is the distance of the ith steel bar from the extreme concrete compressive fibre, ε_{cu} is the ultimate concrete strain, f_{cu} is the compressive concrete cube strength and σ_{max} is the maximum uniaxial concrete stress obtained from concentrically loaded specimens. The contribution of concrete tensile stress to the bending moment capacity is neglected because either the tensile stress of concrete is very small in eccentrically loaded columns or the lever arm from the neutral axis is very small in horizontally loaded columns.

Based on the values of k_3 and c obtained from Equation 3, k_1 and k_2 can be determined from Equations 4a and 4b, respectively

$$\boldsymbol{P} = k_1 k_3 f_{cu} bc + \sum_{i=1}^{n} f_{si}A_{si} \quad \text{4a.}$$

$$\boldsymbol{M} = k_1 k_3 f_{cu} bc\left(\frac{h}{2} - k_2 c\right) + \sum_{i=1}^{n} f_{si}A_{si}\left(\frac{h}{2} - d_i\right) \quad \text{4b.}$$

The obtained values of k_1, k_2, k_3 and c of the eccentrically and horizontally loaded specimens are listed in Table 4 together with their corresponding σ_{max}, ultimate concrete strain ε_{cu} and strain gradient $\phi = \varepsilon_{cu}/c$ (in rad/m). It is evident from the table that

(*a*) the value of k_3 and the product k_1k_3 increase as ϕ increases, which verifies the fact that the strain gradient can improve the maximum concrete stress and concrete force developed in RC members under flexure

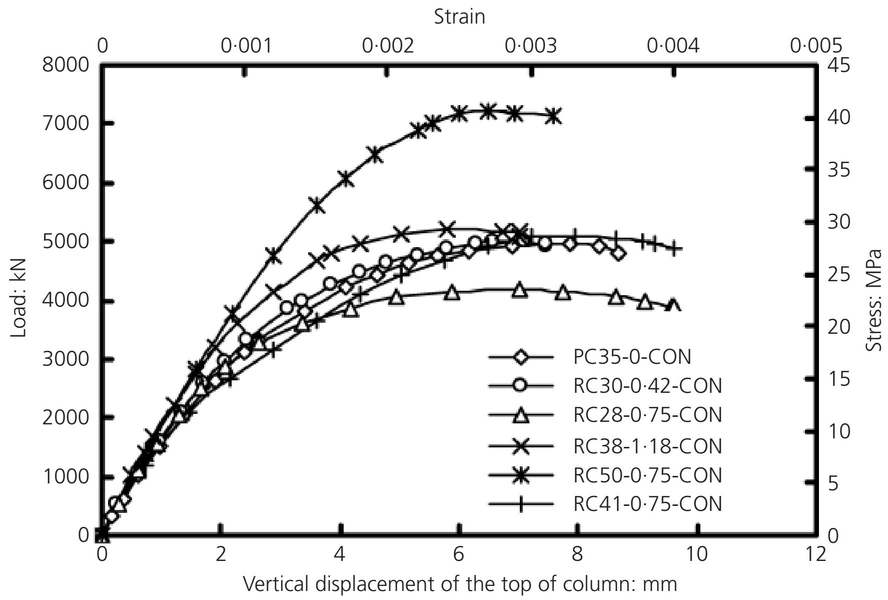

Figure 7. Load–displacement and stress–strain curves of concentrically loaded specimens

(*b*) the values of k_2 are not sensitive to variations in strain gradient.

The obtained values of k_1, k_2 and k_3 obtained from Equations 3 and 4 were averaged and are compared with values obtained by other researchers in Table 5 (Hognestad *et al.*, 1955; Kaar et al., 1978; Mansur *et al.*, 1997; Swartz *et al.*, 1985; Tan and Nguyen, 2004, 2005). The values of k_1 and k_2 obtained in this study agree closely with those obtained by others. However, the values of k_3 and the product k_1k_3 are larger than those obtained in other works. This indicates that the maximum concrete compressive stress and concrete force that can be developed in RC members subjected to flexure with or without axial load should be larger and dependent on strain gradient.

4.2 Derivation of equivalent rectangular stress block parameters α and β

The values of α and β of the equivalent rectangular concrete stress block can be evaluated using Equations 5a and 5b by considering the axial load and moment equilibria in Figure 1(e). The value of α for concentrically loaded specimens can be evaluated using Equation 5c by considering an equivalent concrete stress, αf_{cu}, acting over the concrete cross-section. For eccentric loading

5a. $$\boldsymbol{P} = \alpha\beta f_{\mathrm{cu}}bc + \sum_{i=1}^{n} f_{\mathrm{s}i}A_{\mathrm{s}i}$$

5b. $$\boldsymbol{M} = \alpha\beta f_{\mathrm{cu}}bc\left(\frac{h}{2}-\frac{\beta c}{2}\right) + \sum_{i=1}^{n} f_{\mathrm{s}i}A_{\mathrm{s}i}\left(\frac{h}{2}-d_i\right)$$

and for concentric loading

5c. $$\boldsymbol{P} = \alpha f_{\mathrm{cu}}A_{\mathrm{c}} + \sum_{i=1}^{n} f_{\mathrm{s}i}A_{\mathrm{s}i}$$

Table 6 lists the obtained values of α and β, together with the respective strain gradients ϕ for all specimens. The following conclusion may be drawn from the obtained results.

(*a*) The average value of α obtained from the concentrically loaded columns is about 0·71, which is very close to the design value of $\alpha = 0{\cdot}67$ stipulated in Eurocode 2 (CEN, 2004) (assuming $f'_{\mathrm{c}} = 0{\cdot}8f_{\mathrm{cu}}$).
(*b*) The values of α for specimens subjected to a strain gradient are all larger than 0·67. This implies that strain gradient can enhance the equivalent concrete stress of RC members developed in flexure.
(*c*) The values of α for the eccentrically and horizontally loaded specimens remain fairly constant at low strain gradient, but increase with moderate strain gradient until reaching a maximum limit of about $\alpha \approx 1{\cdot}15$.

It is evident from the above that the variation of α with strain gradient is not linear and is dependent on the value of the strain

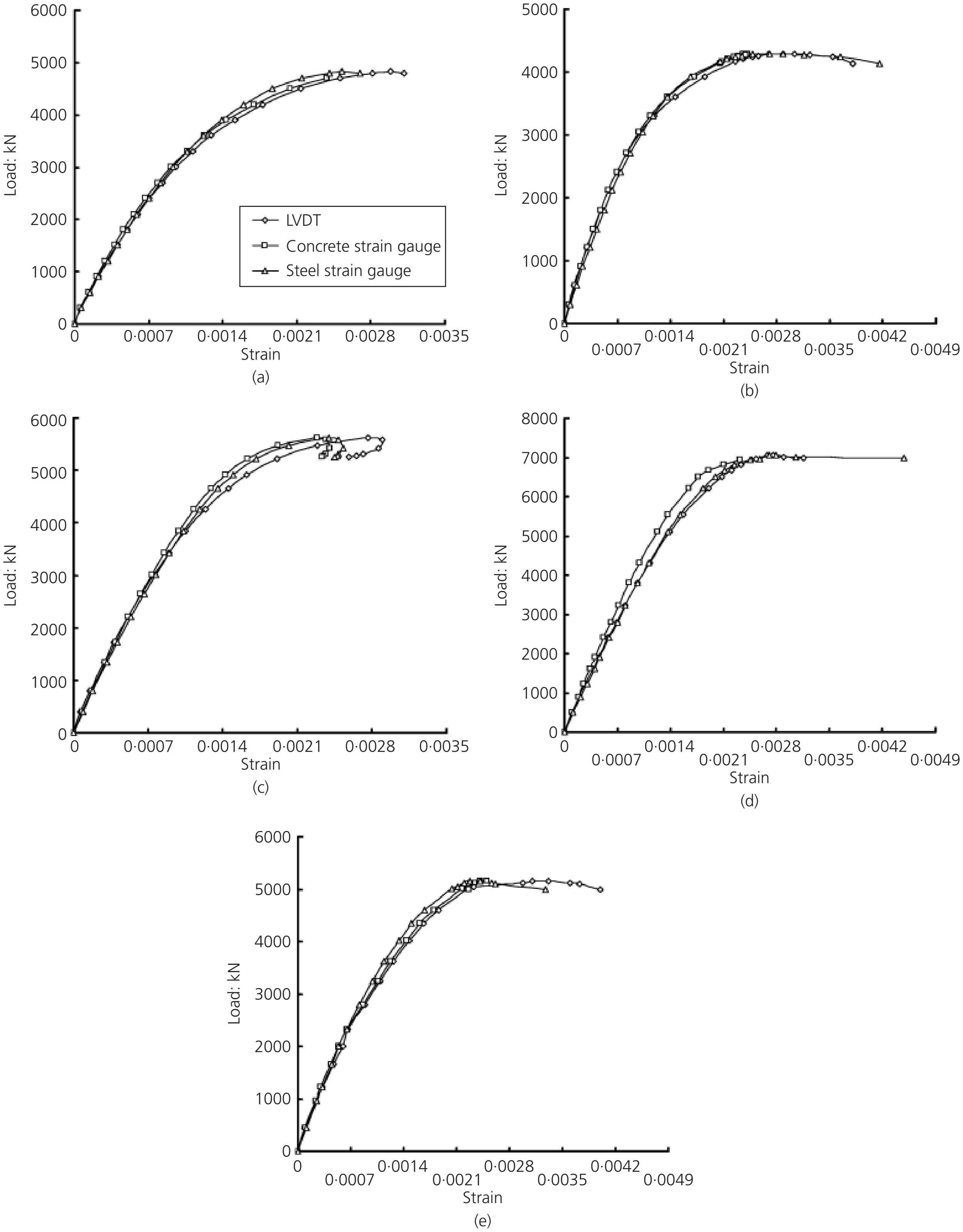

Figure 8. Load–strain curves of concentrically loaded columns: (a) RC30-0·42-CON; (b) RC28-0·75-CON; (c) RC38-1·18-CON; (d) RC50-0·75-CON; (e) RC41-0·75-CON

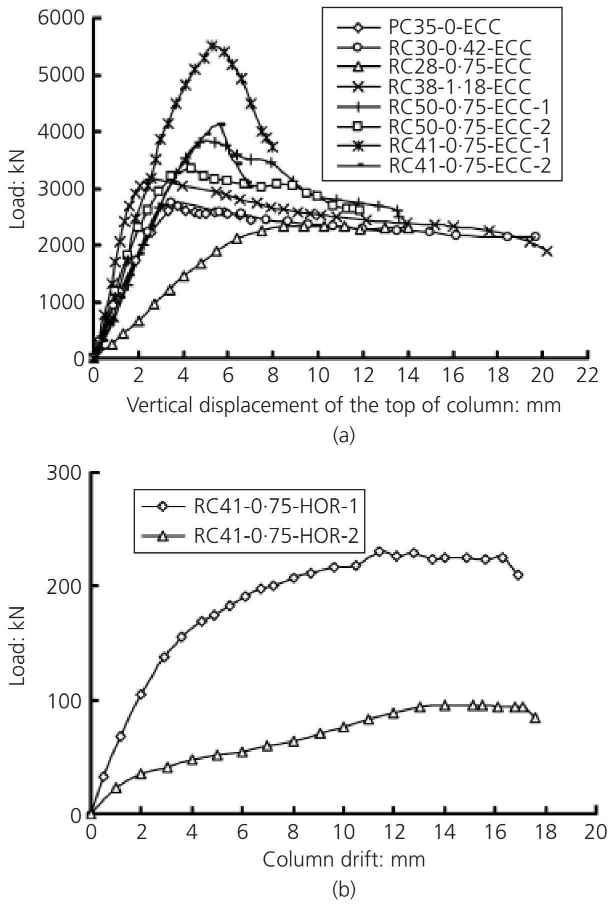

Figure 9. (a) Axial load against vertical displacement for eccentrically loaded specimens. (b) Horizontal load against column drift for horizontally loaded specimens

gradient. This can be reasonably explained by the tests on concrete micro-cracking reported by Sturman *et al.* (1965) who observed that in columns subjected to concentric axial load, extensive micro-cracking of concrete (5 in (127 mm) length) occurred at low concrete strain (0·002) (see Figure 9 in Sturman *et al.* (1965)). Nevertheless, in columns subjected to eccentric axial load, less micro-cracking was observed at the same strain and extensive micro-cracking occurred at larger concrete strains of about 0·0030–0·0035. These observations can logically explain the obtained non-linear variation of equivalent concrete stresses with strain gradient as follows.

(*a*) Initially, when the column was subjected to small strain gradient (i.e. large axial load with a small moment), large concrete cracking occurred at a small concrete strain of about 0·002 and the concrete stress could not be further increased due to crack formation.
(*b*) For columns subjected to larger strain gradient (i.e. medium axial load with a larger moment), significant concrete cracking occurred at a larger concrete strain (0·0030–0·0035). Hence, larger maximum concrete stress was developed because the formation of micro-cracking was delayed.
(*c*) However, for columns subjected to an even larger strain gradient (i.e. low axial load with a very large moment or pure flexure), the maximum concrete stress could not increase further. This is because the strain (0·0030–0·0035) at maximum concrete stress has already reached the ultimate concrete strain, ε_{cu}, which is equal to 0·0035 as per Eurocode 2 (CEN, 2004). At this stage, no further increase in concrete stress should occur; otherwise, the flexural strength of the columns would occur at a much larger strain than ε_{cu}, which

Specimen code	f_{cu}: MPa (testing day)	σ_{max}: MPa	c: mm	k_1	k_2	k_3	k_1k_3	ε_{cu}	ϕ: rad/m	d/c
Plain concrete specimen										
PC35-0-ECC	35·3	28·1	199·2	0·71	0·40	1·33	0·95	0·0035	0·0176	2·01[a]
Reinforced concrete specimens										
RC30-0·42-ECC	35·9	28·1	217·7	0·67	0·40	1·27	0·85	0·0031	0·0142	1·72
RC28-0·75-ECC	31·6	23·5	229·0	0·79	0·39	1·14	0·90	0·0031	0·0135	1·62
RC38-1·18-ECC	42·8	29·3	287·0	0·75	0·40	0·76	0·57	0·0029	0·0101	1·29
RC50-0·75-ECC-1	58·2	40·1	252·0	0·70	0·39	0·90	0·63	0·0035	0·0139	1·44
RC50-0·75-ECC-2	58·2	40·1	223·0	0·68	0·38	0·93	0·63	0·0030	0·0135	1·63
RC41-0·75-ECC-1	49·1	28·7	406·0	0·81	0·38	0·76	0·61	0·0033	0·0081	0·90
RC41-0·75-ECC-2	49·1	28·7	234·0	0·84	0·38	0·96	0·81	0·0033	0·0141	1·56
RC41-0·75-HOR-1	46·4	28·7	76·0	0·66	0·38	1·29	0·84	0·0033	0·0434	4·79
RC41-0·75-HOR-2	46·4	28·7	27·0	0·66	0·38	1·31	0·86	0·0028	0·1148	13·48
Average	46·0	30·4	—	0·73	0·40	1·02	0·76	0·0031	—	—

[a] *d* is effective depth of RC specimens and is taken as the overall depth of column for the PC specimen

Table 4. Obtained values of k_1, k_2 and k_3

Research	f'_c: MPa	k_1	k_2	k_3	k_1k_3
Hognestad *et al.* (1955)	27·6	0·79	0·45	0·94	0·74
Hognestad *et al.* (1955)	34·5	0·75	0·44	0·92	0·69
Kaar *et al.* (1978)	45·0	0·72	0·40	0·97	0·70
Mansur *et al.* (1997)	57·2	0·70	0·42	0·98	0·69
Swartz *et al.* (1985)	57·0	0·71	0·42	0·98	0·70
Tan and Nguyen (2004, 2005)	48·3	0·70	0·38	0·93	0·65
Current work	46·0[a]	0·73	0·40	1·02	0·76

[a] f_{cu} (in MPa)

Table 5. Comparisons of k_1, k_2 and k_3

Specimen code	α	β	ε_{cu}	ϕ: rad/m	*d/c*
PC35-0-CON	0·80	—	—	0·0	0·0
RC30-0·42-CON	0·66	—	—	0·0	0·0
RC28-0·75-CON	0·70	—	—	0·0	0·0
RC38-1·18-CON	0·68	—	—	0·0	0·0
RC50-0·75-CON	0·76	—	—	0·0	0·0
RC41-0·75-CON	0·68	—	—	0·0	0·0
Average	0·71	—	—	0·0	0·0
PC35-0-ECC	1·18	0·80	0·0035	0·0176	2·01[a]
RC30-0·42-ECC	1·06	0·81	0·0031	0·0142	1·72
RC28-0·75-ECC	1·15	0·78	0·0031	0·0135	1·62
RC38-1·18-ECC	0·72	0·79	0·0029	0·0101	1·29
RC50-0·75-ECC-1	0·80	0·79	0·0035	0·0139	1·44
RC50-0·75-ECC-2	0·82	0·77	0·0030	0·0135	1·63
RC41-0·75-ECC-1	0·80	0·76	0·0033	0·0081	0·90
RC41-0·75-ECC-2	1·07	0·76	0·0033	0·0141	1·56
RC41-0·75-HOR-1	1·10	0·77	0·0033	0·0434	4·79
RC41-0·75-HOR-2	1·15	0·75	0·0028	0·1148	13·48
Average	—	0·78	0·0031	—	—

[a] *d* is effective depth of RC specimens and is taken as the overall depth of column for the PC specimen

Table 6. Obtained values of equivalent rectangular stress block parameters and strain gradient

has never been observed in previous experimental tests for unconfined columns.

From the above comparison, it is believed that the current design codes can predict fairly accurately the strengths of RC columns subjected to pure axial load without strain gradient, but underestimate the strengths of RC beams and columns subjected to flexure with or without axial load. This is because the equivalent rectangular concrete stress that is currently adopted for flexural strength design does not take into account the enhancement of concrete stress due to the strain gradient effect.

5. Modification of stress block parameters by incorporating strain gradient effects

The stress block parameters of k_1, k_2, k_3, α and β obtained in this study are summarised in Tables 4 and 6, together with their corresponding strain gradients $\phi = \varepsilon_{cu}/c$ (rad/m). However, since ϕ is non-dimensionless, the formula that correlates these stress block parameters to ϕ will include the effect of column dimensions. In order to eliminate the column size effect, a dimensionless factor, d/c, is proposed to replace ϕ to represent strain gradient, where d and c are effective and neutral axis depths respectively. To investigate the relationships of k_1, k_2, k_3, α and β with strain gradient in dimensionless form, the values of these parameters obtained in the present study are plotted against d/c in Figures 10 and 11. It is apparent from Figures 10(a), 10(b) and 11(b) that k_1, k_2 and β remain fairly constant at 0·73, 0·40 and 0·80, respectively. However, Figures 10(c) and 11(a) show that k_3 and α increase with strain gradient in a tri-linear manner. Two formulas are thus proposed to correlate k_3 and α with strain gradient using linear regression analysis

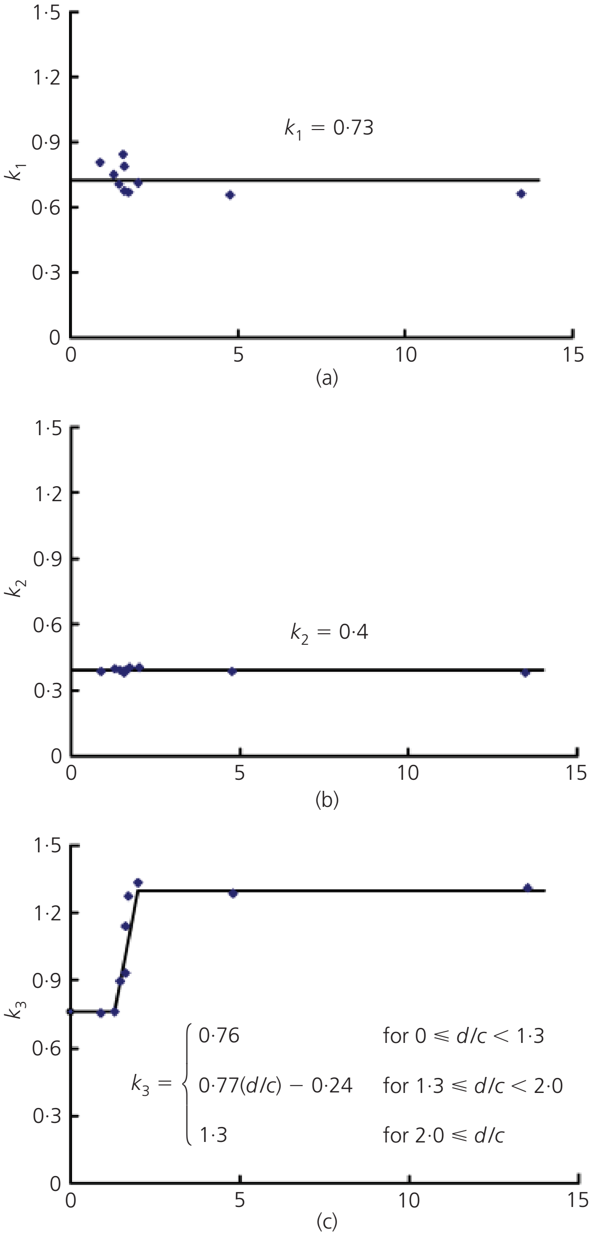

Figure 10. Relationships of k_1, k_2 and k_3 with strain gradient d/c

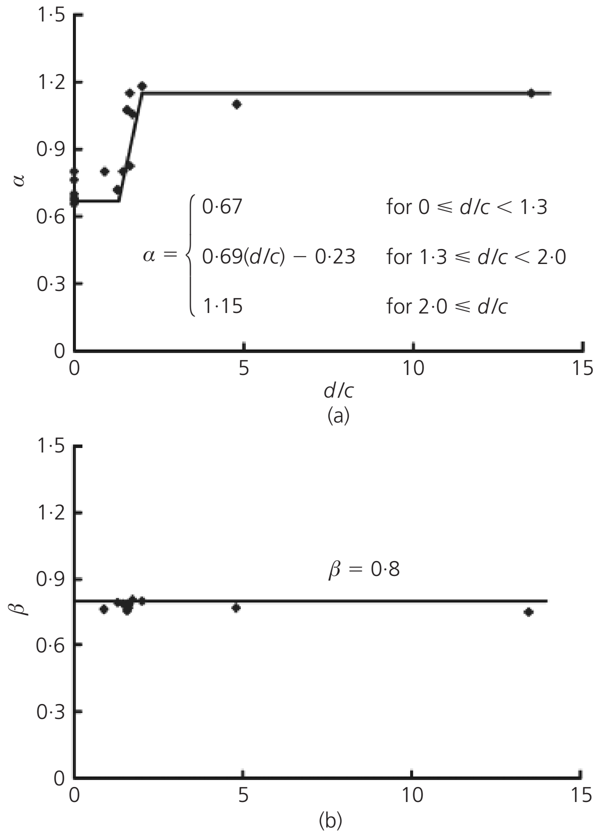

Figure 11. Relationships of α and β with strain gradient d/c

6. $$k_3 = \begin{cases} 0{\cdot}76 & \text{for } 0 \leqslant d/c < 1{\cdot}3 \\ 0{\cdot}77(d/c) - 0{\cdot}24 & \text{for } 1{\cdot}3 \leqslant d/c < 2{\cdot}0 \\ 1{\cdot}3 & \text{for } 2{\cdot}0 \leqslant d/c \end{cases}$$

7. $$\alpha = \begin{cases} 0{\cdot}67 & \text{for } 0 \leqslant d/c < 1{\cdot}3 \\ 0{\cdot}69(d/c) - 0{\cdot}23 & \text{for } 1{\cdot}3 \leqslant d/c < 2{\cdot}0\,.. \\ 1{\cdot}15 & \text{for } 2{\cdot}0 \leqslant d/c \end{cases}$$

For the obtained value of $k_2 = 0{\cdot}40$, the following fixed value of β is proposed

8. $$\beta = 2k_2 = 2 \times 0{\cdot}4 = 0{\cdot}8$$

From Table 4, the value of ultimate concrete strain for design is taken as $\varepsilon_{cu} = 0{\cdot}0031$.

Specimen code	$f'_c = 0{\cdot}8f_{cu}$: MPa	Moment: kNm					$\frac{(1)}{(5)}$	$\frac{(2)}{(5)}$	$\frac{(3)}{(5)}$	$\frac{(4)}{(5)}$
		M_p (1)	M_{ACI} (2)	M_{EC} (3)	M_{NZ} (4)	M_t (5)				
Pecce and Fabbrocino (1999)										
A	41·3	103·8	97·0	97·0	97·0	104·0	1·00	0·93	0·93	0·93
B	41·3	46·8	45·0	45·0	45·0	49·6	0·94	0·91	0·91	0·91
C	42·3	693·4	636·7	636·7	636·7	712·5	0·97	0·89	0·89	0·89
Ashour (2000)										
B-N2	48·6	55·4	53·6	53·6	53·6	58·2	0·95	0·92	0·92	0·92
B-N3	48·6	81·1	77·1	77·1	77·1	80·6	1·01	0·96	0·96	0·96
B-N4	48·6	105·6	98·4	98·4	98·4	99·6	1·06	0·99	0·99	0·99
Pam *et al.* (2001)										
1	29·9	58·3	56·1	56·1	56·1	77·6	0·75	0·72	0·72	0·72
2	29·4	85·0	80	80·0	80	103·5	0·82	0·77	0·77	0·77
3	29·1	128·5	114·1	111·5	114·1	126·5	1·02	0·90	0·88	0·90
4	33·8	122·6	112·0	112·7	112·0	129·0	0·95	0·87	0·87	0·87
5	37·1	148·4	133·8	134·8	133·8	142·8	1·04	0·94	0·94	0·94
6	34·6	173·9	144·8	139·6	144·8	162·0	1·07	0·89	0·86	0·89
7	46·9	158·4	145·7	162·3	145·7	164·6	0·96	0·89	0·89	0·89
8	45·7	176·8	160·6	161·4	160·6	166·2	1·06	0·97	0·97	0·97
Debernardi and Taliano (2002)										
T1	27·7	11·1	10·8	10·8	10·8	13·6	0·82	0·79	0·79	0·79
T2	27·7	21·3	20·5	20·6	20·5	23·6	0·90	0·87	0·87	0·87
T3	27·7	30·9	28·9	29·3	28·9	32·5	0·95	0·89	0·90	0·89
T4	27·7	48·7	46·9	46·8	46·9	59·8	0·81	0·78	0·78	0·78
T5	27·7	92·6	93·1	93·1	93·1	107·5	0·86	0·87	0·87	0·87
T6	27·7	176·9	170·5	171·2	170·5	192·4	0·92	0·89	0·89	0·89
T7	27·7	242·0	217·2	221·7	217·2	221·6	1·09	0·98	1·00	0·98
T8	27·7	81·4	81·1	81·2	81·1	93·9	0·87	0·86	0·86	0·86
T9	27·7	152·0	152·0	151·9	152·0	182·7	0·83	0·83	0·83	0·83
T10	27·7	322·9	324·6	324·7	324·6	330·4	0·98	0·98	0·98	0·98
Lam *et al.* (2008)										
L-C1	29·8	15·0	14·6	14·6	14·6	14·2	1·06	1·03	1·03	1·03
L-D	29·8	10·1	9·8	9·8	9·8	11·6	0·87	0·84	0·84	0·84
L-E	29·8	30·1	25·9	26·0	25·9	29·4	1·02	0·88	0·89	0·88
Fathifazl *et al.* (2009)										
EV-1·5N	43·5	83·4	79·4	79·5	79·4	86·9	0·96	0·91	0·91	0·91
EV-2·7N	43·5	113·4	108·3	108·4	108·3	126·4	0·90	0·86	0·86	0·86
CG-2·7N	43·5	112·9	106·3	106·3	106·3	118·5	0·95	0·90	0·90	0·90
Average							0·95	0·89	0·90	0·89

Table 7. Proposed strength comparisons of beams

6. Verification of the proposed stress block parameters

The applicability of the proposed stress block parameters (i.e. α, β and ε_{cu}) was verified by comparing the measured flexural strengths obtained experimentally by other researchers. The flexural strengths predicted using the proposed stress block parameters, $\boldsymbol{M}_p$, were compared with experimentally measured strengths, $\boldsymbol{M}_t$, and the strengths calculated using various RC design codes (i.e. $\boldsymbol{M}_{ACI}$ based on ACI 318 (ACI, 2008), $\boldsymbol{M}_{EC}$ based on Eurocode 2 (CEN, 2004) and $\boldsymbol{M}_{NZ}$ based on NZS 3101 (SNZ, 2006). The comparisons are shown in Tables 7 to 11.

Table 7 shows the strength comparison of beams subjected to pure flexure (Ashour, 2000; Debernardi and Taliano, 2002; Fathifazl *et al.*, 2009; Lam *et al.*, 2008; Pam *et al.*, 2001; Pecce and Fabbrocino, 1999), while Tables 8 to 11 show the strength comparisons of columns subjected to low axial load ($0 < \boldsymbol{P}/A_g f'_c \leqslant 0{\cdot}2$) (Marefat *et al.*, 2005; Mo and Wang, 2000; Tao and Yu, 2008; Watson and Park, 1994), medium axial load ($0{\cdot}2 < \boldsymbol{P}/A_g f'_c \leqslant 0{\cdot}5$) (Lam *et al.*, 2003; Marefat *et al.*, 2005, 2006; Mo and Wang, 2000; Sheikh and Khoury, 1993; Tao and Yu, 2008; Watson and Park, 1994), high axial load ($0{\cdot}5 < \boldsymbol{P}/A_g f'_c \leqslant 0{\cdot}7$) (Ho and Pam, 2003; Lam *et al.*, 2003; Sheikh and Yeh, 1990; Sheikh *et al.*, 1994; Watson and Park, 1994) and ultra-high axial load level ($0{\cdot}7 < \boldsymbol{P}/A_g f'_c$) (Nemecek *et al.*, 2005; Sheikh and Khoury, 1993; Sheikh and Yeh, 1990; Sheikh *et al.*, 1994) (**P** is compressive axial load, A_g is the gross area of concrete and f'_c is the concrete cylinder strength). It should be noted that the concrete cylinder strengths reported by other researchers were converted to cube strength using $f'_c = 0{\cdot}8 f_{cu}$ in the comparison. From the tables, the following conclusions may be drawn.

(*a*) The flexural strength evaluated with the proposed equivalent rectangular stress block parameters α, β and ε_{cu}, which take into account the strain gradient effects, results in a better estimation than that predicted by the current design codes for RC beams and columns subjected to low and medium axial load levels.
(*b*) For RC columns subjected to high and ultra-high axial load levels, the flexural strengths evaluated with α, β and ε_{cu}, are similar to those predicted by current design codes.

Specimen code	$f'_c = 0{\cdot}8 f_{cu}$: MPa	$P/A_g f'_c$	Moment: kNm					$\frac{(1)}{(5)}$	$\frac{(2)}{(5)}$	$\frac{(3)}{(5)}$	$\frac{(4)}{(5)}$
			M_p (1)	M_{ACI} (2)	M_{EC} (3)	M_{NZ} (4)	M_t (5)				
Watson and Park (1994)											
1	47·0	0·100	323·5	302·0	306·9	302·0	335·2	0·97	0·90	0·92	0·90
Mo and Wang (2000)											
C1-1	24·9	0·113	335·3	300·5	305·1	300·5	351·4	0·95	0·86	0·87	0·86
C1-2	26·7	0·106	340·1	303·8	308·2	303·8	374·6	0·91	0·81	0·82	0·81
C1-3	26·1	0·108	338·0	302·8	307·2	302·8	427·7	0·79	0·71	0·72	0·71
C2-1	25·3	0·167	361·0	319·1	326·8	319·1	347·3	1·04	0·92	0·94	0·92
C2-2	27·1	0·156	365·6	325·2	330·5	325·2	399·9	0·92	0·81	0·83	0·81
C2-3	26·8	0·158	364·5	324·4	329·7	324·4	427·2	0·85	0·76	0·77	0·76
Marefat *et al.* (2005)											
STCM-9	24·0	0·190	25·7	22·8	22·5	22·5	23·3	1·10	0·97	0·98	0·97
SBCC-7	27·0	0·160	43·5	41·6	41·9	41·7	45·1	0·96	0·92	0·93	0·92
Tao and Yu (2008)											
US-3U	49·2	0·108	17·9	16·5	16·5	16·5	15·9	1·13	1·04	1·04	1·04
BS-3U	49·8	0·098	16·7	15·4	15·4	15·4	14·6	1·14	1·05	1·05	1·05
BS-4U	49·8	0·067	14·9	13·6	13·7	13·6	13·3	1·12	1·02	1·03	1·02
Average								0·99	0·90	0·91	0·90

Table 8. Proposed strength comparisons of columns subjected to low axial load level

Specimen code	$f'_c = 0{\cdot}8f_{cu}$: MPa	$P/A_g f'_c$	Moment: kNm					$\frac{(1)}{(5)}$	$\frac{(2)}{(5)}$	$\frac{(3)}{(5)}$	$\frac{(4)}{(5)}$
			M_p (1)	M_{ACI} (2)	M_{EC} (3)	M_{NZ} (4)	M_t (5)				
Sheikh and Khoury (1993)											
AS-19	32·3	0·470	234·4	178·5	183·9	179·2	219·7	1·06	0·81	0·84	0·82
Watson and Park (1994)											
2	44·0	0·300	493·3	405·9	410·2	406·0	486·0	1·02	0·84	0·84	0·84
3	44·0	0·300	493·3	405·9	410·2	406·0	479·1	1·03	0·85	0·86	0·85
4	40·0	0·300	462·6	382·1	385·3	382·3	448·1	1·03	0·85	0·86	0·85
5	41·0	0·500	572·8	372·9	383·2	373·4	525·8	1·09	0·71	0·73	0·71
6	40·0	0·500	562·4	367·2	376·7	367·8	526·4	1·07	0·70	0·72	0·70
Mo and Wang (2000)											
C3-1	26·4	0·213	386·9	333·3	343·9	333·3	353·4	1·10	0·94	0·97	0·94
C3-2	27·5	0·205	390·4	337·7	348·2	337·7	395·5	0·99	0·85	0·88	0·85
C3-3	26·9	0·209	388·2	335·4	345·9	335·4	423·8	0·92	0·79	0·82	0·79
Lam *et al.* (2003)											
X6	31·9	0·450	33·1	28·5	29·0	28·6	37·1	0·89	0·77	0·78	0·77
X7	35·7	0·450	36·7	29·7	30·5	29·8	37·1	0·99	0·80	0·82	0·80
Marefat *et al.* (2005)											
NTCM-14	20·1	0·310	18·7	16·0	16·0	16·0	16·8	1·11	0·95	0·95	0·95
NBCC-12	25·2	0·230	22·5	22·0	22·4	22·0	21·7	1·04	1·01	1·03	1·01
NBCM-11	24·5	0·250	46·8	38·6	38·5	38·6	44·6	1·05	0·87	0·86	0·87
SBCM-8	28·0	0·220	52·4	46·0	46·0	46·0	58·7	0·89	0·78	0·78	0·78
Marefat *et al.* (2006)											
NTMM-13	21·0	0·310	19·1	16·3	16·4	16·3	17·3	1·10	0·94	0·95	0·94
Tao and Yu (2008)											
BS-2U	49·8	0·230	24·2	21·7	21·8	21·7	25·1	0·96	0·86	0·87	0·86
Average								1·02	0·84	0·85	0·84

Table 9. Proposed strength comparisons of columns subjected to medium axial load level

(*c*) For RC beams, the average ratio of the predicted to experimentally measured flexural strength is 0·95, whereas the average ratio of the code-predicted to measured strength is 0·89. Therefore, it is evident that the proposed stress block parameters can improve the accuracy of flexural strength prediction by 6% on average.

(*d*) For RC columns subjected to low and medium axial load levels, the average ratios of the predicted to experimentally measured flexural strength are 0·99 and 1·02, respectively, whereas the average ratios of the code-predicted to measured strengths are 0·90 and 0·84, respectively. The proposed stress block method can thus improve the accuracy of flexural strength prediction by 9% and 18% on average.

(*e*) For RC columns subjected to high and ultra-high axial load levels, the average ratios of the predicted to experimentally measured flexural strength are 0·86 and 0·92, respectively,

Specimen code	$f'_c = 0{\cdot}8f_{cu}$: MPa	$P/A_g f'_c$	Moment: kNm					$\frac{(1)}{(5)}$	$\frac{(2)}{(5)}$	$\frac{(3)}{(5)}$	$\frac{(4)}{(5)}$
			M_p (1)	M_{ACI} (2)	M_{EC} (3)	M_{NZ} (4)	M_t (5)				
Sheikh and Yeh (1990)											
E-2	31·4	0·610	152·3	160·1	163·5	160·5	169·3	0·89	0·95	0·97	0·95
A-3	31·8	0·610	151·3	162·7	161·9	163·1	197·8	0·77	0·82	0·82	0·82
F-4	32·2	0·600	155·1	164·8	168·0	165·2	198·4	0·78	0·83	0·85	0·83
F-12	33·4	0·600	155·1	156·1	157·9	156·5	161·1	0·96	0·97	0·98	0·97
A-16	33·9	0·600	156·0	157·1	159·1	157·6	157·5	0·99	1·00	1·01	1·00
Sheikh *et al.* (1994)											
AS-3	33·2	0·600	154·2	167·1	169·3	167·5	192·9	0·80	0·87	0·88	0·87
AS-3H	54·1	0·620	203·0	208·6	210·2	208·3	237·4	0·86	0·88	0·89	0·88
Watson and Park (1994)											
7	42·0	0·700	537·7	430·3	434·0	430·3	516·8	1·02	0·83	0·84	0·83
8	39·0	0·700	529·2	407·7	411·4	407·7	524·5	1·01	0·77	0·78	0·77
Ho and Pam (2003)											
BS-60-06-61-S	51·1	0·675	361·9	373·4	400·7	373·0	417·7	0·86	0·89	0·96	0·89
BS-60-06-61-S	53·2	0·647	368·5	384·7	405·6	376·4	426·7	0·86	0·90	0·95	0·88
Lam *et al.* (2003)											
X4	31·9	0·650	23·7	24·3	24·6	24·9	34·5	0·69	0·71	0·71	0·72
X5	31·9	0·650	23·7	24·3	24·6	24·9	36·3	0·65	0·67	0·68	0·69
Average								0·86	0·86	0·88	0·86

Table 10. Proposed strength comparisons of columns subjected to high axial load level

whereas the average ratios of the code- predicted to measured strengths are 0·87 and 0·95, respectively. The proposed stress block method, therefore, gives the same accuracy as the current codes in predicting flexural strength.

7. Conclusion

A total of 16 inverted T-shaped specimens were fabricated and tested to investigate the effects of strain gradient on the maximum and equivalent concrete stresses that can be developed in RC members under flexure. The specimens were divided into six groups, each of which consisted of columns with identical section properties and material strengths. One of the specimens in each group was concentrically loaded while the rest was/were eccentrically or horizontally loaded. Strain gradient effects on the maximum concrete stress were studied using k_3, the ratio of the maximum concrete stress developed under flexure to the concrete cube strength.

The effect of strain gradient on the equivalent concrete stress developed under flexure was investigated using the parameter α, the ratio of the equivalent concrete stress to concrete cube strength.

The effects of strain gradient on the maximum and equivalent concrete stresses developed in flexure were studied by modifying the uniaxial stress–strain curve of concrete obtained from the concentrically loaded specimen, based on which the axial load and moment capacities evaluated for the eccentrically or horizontally loaded specimen were matched with the experimentally measured values. From the results obtained, it was found that the values of k_3 and α are larger than those obtained by

Specimen code	$f'_c = 0{\cdot}8 f_{cu}$: MPa	$P/A_g f'_c$	Moment: kNm					$\frac{(1)}{(5)}$	$\frac{(2)}{(5)}$	$\frac{(3)}{(5)}$	$\frac{(4)}{(5)}$
			M_p (1)	M_{ACI} (2)	M_{EC} (3)	M_{NZ} (4)	M_t (5)				
Sheikh and Yeh (1990)											
F-6	27·2	0·750	126·3	133·5	134·7	133·5	145·4	0·87	0·92	0·93	0·92
D-7	26·2	0·780	116·2	121·0	123·1	121·0	133·3	0·87	0·91	0·92	0·91
E-8	25·9	0·780	121·0	128·4	129·2	128·4	129·2	0·94	0·99	1·00	0·99
F-9	26·5	0·770	123·8	130·9	131·6	130·9	152·0	0·82	0·86	0·87	0·86
E-10	26·3	0·770	121·9	130·6	131·3	130·6	132·7	0·91	0·98	0·99	0·98
A-11	27·9	0·740	130·6	139·1	139·7	139·1	135·2	0·96	1·03	1·03	1·03
E-13	27·2	0·740	126·7	134·9	136·2	134·9	128·0	0·99	1·05	1·06	1·05
D-14	26·9	0·750	122·9	126·9	128·8	126·9	116·5	1·05	1·09	1·11	1·09
D-15	26·2	0·750	123·8	124·6	124·6	124·1	134·5	0·92	0·93	0·93	0·92
Sheikh and Khoury (1993)											
ES-13	32·5	0·760	130·7	139·8	141·2	140·0	163·3	0·80	0·86	0·86	0·86
FS-9	32·4	0·760	129·7	139·6	141·0	139·9	157·2	0·83	0·89	0·90	0·89
Sheikh *et al.* (1994)											
AS-17	31·3	0·770	128·3	136·2	137·4	136·4	180·2	0·71	0·76	0·76	0·76
Nemecek *et al.* (2005)											
N50	30·0	0·915	9·9	9·5	10·9	9·4	9·6	0·94	0·99	1·14	0·98
N100	30·0	0·900	10·1	9·9	11·4	9·9	9·3	1·08	1·06	1·23	1·06
N150	30·0	0·892	10·2	10·2	11·6	10·1	9·3	1·09	1·10	1·25	1·09
Average								0·92	0·96	1·00	0·90

Table 11. Proposed strength comparisons of columns subjected to ultra-high axial load level

previous researchers and those specified in current RC design codes. More importantly, it was found that k_3 and α are dependent on strain gradient but the variations are non-linear. The values of k_3 and α remain relatively constant at low strain gradient, but increase significantly with moderate strain gradient until they reach the maximum limits of about 1·3 and 1·15 respectively. It was also found that the values of α for concentrically loaded columns are very similar to those specified in the current design codes.

Based on the obtained values of k_3 and α, empirical formulas were proposed for k_3 and α that incorporate strain gradient effects; the values of the other stress block parameters, k_1, k_2, β and ε_{cu}, were found to remain relatively constant at about 0·73, 0·40, 0·80 and 0·0031 respectively. In order to verify the applicability of the proposed equivalent rectangular stress block parameters, they were used to predict the flexural strengths of RC beams and columns subjected to various axial load levels in tests carried out by previous researchers. The predicted strengths were compared with experimental strengths and theoretical strengths calculated using current RC design codes. The comparisons show that the proposed strain-gradient-dependent equivalent concrete stress block is more accurate in predictions of the flexural strength of RC beams and columns subjected to low and medium axial load levels than current codes. The improvements are 6% for RC beams and 18% for columns subjected to a medium axial load level. However, the proposed parameters do not improve the flexural strength prediction of RC columns subjected to high and ultra-high axial load levels because the strain gradient developed in these columns is very small.

Lastly, it is worth noting that this paper has only considered the beneficial effects of strain gradient on the flexural strength design of RC beams and columns; it does not comment on the suitability of implementing the proposed equations on α and β in existing design codes. This is because the current study did not consider any variability (e.g. material strength) and uncertainty, which should also be taken into account when establishing design clauses.

Acknowledgements

A research grant from the Seed Funding Programme for Basic Research (account code 10401445) of The University of Hong Kong (HKU) for the work presented here is gratefully acknowledged. The authors gratefully thank the Department of Civil and Structural Engineering, Hong Kong Polytechnic University (PolyU), where most of the experimental tests were conducted. The support of the technical staff in the structural laboratory of PolyU and the Department of Civil Engineering of HKU is also greatly appreciated.

REFERENCES

ACI (American Concrete Institute) (2008) ACI 318: Building code requirements for reinforced concrete and commentary ACI 318M-08. ACI, Farmington Hills, MI, USA.

Ahn JM and Shin SW (2007) An evaluation of ductility of high-strength reinforced concrete columns subjected to reverse cyclic loads under axial compression. *Magazine of Concrete Research* **59(1)**: 29–44.

Ashour SA (2000) Effect of compressive strength and tensile reinforcement ratio on flexural behaviour of high-strength concrete beams. *Engineering Structures* **25(8)**: 1083–1096.

Arslan G (2010) Shear strength of reinforced concrete slender beams. *Proceedings of the Institution of Civil Engineers – Structures and Buildings* **163(3)**: 195–205.

Arslan MH, Yuksel I and Kaltakci MY (2010) An investigation on global ductility of strengthened RC frames, *Proceedings of the Institution of Civil Engineers – Structures and Buildings* **163(3)**: 177–194.

Baczkowski BJ and Kuang JS (2008) A new approach to testing concrete coupling beams subjected to reversed cyclic loading. *Magazine of Concrete Research* **60(4)**: 301–309.

Bai ZZ and Au FTK (2008) Ductility of symmetrically reinforced concrete columns. *Magazine of Concrete Research* **61(5)**: 345–357.

Bukhari IA, Vollum RL, Ahmad S and Sagaseta J (2010) Shear strengthening of reinforced concrete beams with CFRP. *Magazine of Concrete Research* **62(1)**: 65–77.

CEN (European Committee for Standardization) (2004) BS EN 1992: Eurocode 2: Design of concrete structures. Part 1-1: general rules and rules for buildings. CEN, Brussels, Belgium.

Chen Y and May IM (2009) Reinforced concrete members under drop-weight impacts. *Proceedings of the Institution of Civil Engineers – Structures and Buildings* **162(1)**: 45–56.

Choi E, Park J, Nam TH and Yoon SJ (2009) A new steel jacketing method for RC columns. *Magazine of Concrete Research* **61(10)**: 787–796.

Clark LE, Gerstle KH and Tulin LG (1967) Effect of strain gradient on the stress–strain curve of mortar and concrete. *ACI Journal* **64(50)**: 580–586.

Debernardi PG and Taliano M (2002) On evaluation of rotation capacity for reinforced concrete beams. *ACI Structural Journal* **99(3)**: 360–368.

Do Carmo RNF and Lopes SM (2006) Required plastic rotation of RC beams. *Proceedings of the Institution of Civil Engineers – Structures and Buildings* **159(2)**: 77–85.

Fathifazl G, Razaqpur AG, Isgor OB *et al.* (2009) Shear strength of reinforced recycled concrete beams without stirrups. *Magazine of Concrete Research* **61(7)**: 477–490.

Han TH, Stallings JM, Cho SK and Kang YJ (2010) Behaviour of a hollow RC column with an internal tube. *Magazine of Concrete Research* **62(1)**: 25–38.

Ho JCM and Pam HJ (2003) Influence of transverse steel configuration on post-elastic behaviour of high-strength reinforced concrete columns. *Transactions of the Hong Kong Institution of Engineers* **10(2)**: 1–9.

Ho JCM and Pam HJ (2010) Deformability evaluation of high-strength reinforced concrete columns. *Magazine of Concrete Research* **62(8)**: 569–583.

Hognestad E (1957) Confirmation of inelastic stress distribution in concrete. *Proceedings of ASCE* **83(2)**: 1–17.

Hognestad E, Hanson NW and McHenry D (1955) Concrete stress distribution in ultimate strength design. *ACI Journal* **52(4)**: 455–479.

Ibrahim HHH and MacGregor JG (1996) Flexural behavior of laterally reinforced high-strength concrete sections. *ACI Structural Journal* **93(6)**: 674–684.

Ibrahim HHH and MacGregor JG (1997) Modification of the ACI rectangular stress block for high-strength concrete. *ACI Structural Journal* **94(1)**: 40–48.

Inel M, Aschheim MA and Pantazopoulou SJ (2007) Seismic deformation capacity indices for concrete columns: model estimates and experimental results. *Magazine of Concrete Research* **59(4)**: 297–310.

Inel M, Bilgin H and Ozmen HB (2008) Seismic capacity evaluation of school buildings in Turkey. *Proceedings of the Institution of Civil Engineers – Structures and Buildings* **161(3)**: 147–159.

Jaafar K (2008) Shear behaviour of reinforced concrete beams with confinement near plastic hinges. *Magazine of Concrete Research* **60(9)**: 665–672.

Jones J and Fraser R (2009) Ship impact on concrete offshore platform legs. *Proceedings of the Institution of Civil Engineers – Structures and Buildings* **162(1)**: 21–25.

Kaar PH, Hanson NW and Capell HT (1978) Stress–strain characteristics of high strength concrete. *Douglas McHenry International Symposium on Concrete and Concrete Structures*. American Concrete Institute, Farmington Hills, MI, USA, pp. 161–185.

Kim TH, Kim YJ and Shin HM (2007) Seismic performance assessment of reinforced concrete bridge columns under variable axial load. *Magazine of Concrete Research* **59(2)**: 87–96.

Kriz LB (1959) Ultimate strength criteria for reinforced concrete. *Proceedings of ASCE* **85(3)**: 95–110.

Lam SSE, Wu B, Wong YL *et al.* (2003) Drift capacity of rectangular reinforced concrete columns with low lateral confinement and high-axial load. *Journal of Structural Engineering ASCE* **129(6)**: 733–742.

Lam SSE, Wu B, Liu ZQ and Wong YL (2008) Experimental study on seismic performance of coupling beams not designed for ductility. *Structural Engineering and Mechanics* **28(3)**: 317–333.

Lu WY, Lin IJ and Hwang SJ (2009) Shear strength of reinforced concrete corbels. *Magazine of Concrete Research* **61(10)**: 807–813.

Marefat MS, Khanmohammadi M, Bahrani MK and Goli A (2005) Cyclic load testing and numerical modelling of concrete columns with substandard seismic details. *Computers and Concrete* **2(5)**: 367–380.

Marefat MS, Khanmohammadi M, Bahrani MK and Goli A (2006) Experimental assessment of reinforced concrete columns with deficient seismic details under cyclic load. *Advances in Structural Engineering* **9(3)**: 337–347.

Mansur MA, Chin MS and Wee TH (1997) Flexural behavior of high-strength concrete beams. *ACI Structural Journal* **94(6)**: 663–673.

Mattock AH, Kriz LB and Hognestad E (1961) Rectangular concrete stress distribution in ultimate strength design. *ACI Journal* **32(8)**: 875–927.

Mo YL and Wang SJ (2000) Seismic behavior of RC columns with various tie configurations. *Journal of Structural Engineering, ASCE* **126(10)**: 1122–1130.

Nemecek P, Padevet B, Patzak B and Bittnar Z (2005) Effect of transversal reinforcement in normal and high strength concrete columns. *Materials and Structures* **38(7)**: 665–671.

Oehlers DJ, Haskett M, Mohamed Ali MS and Griffith MC (2010) Moment redistribution in reinforced concrete beams, *Proceedings of the Institution of Civil Engineers – Structures and Buildings* **163(3)**: 165–176.

Pam HJ and Ho JCM (2001) Flexural strength enhancement of confined reinforced concrete columns. *Proceedings of the Institution of Civil Engineers – Structures and Buildings* **146(4)**: 363–370.

Pam HJ and Ho JCM (2009) Length of critical region for confinement steel in limited ductility high-strength reinforced concrete columns. *Engineering Structures* **31(12)**: 2896–2908.

Pam HJ, Kwan AKH and Islam MS (2001) Flexural strength and ductility of reinforced normal- and high-strength concrete beams. *Proceedings of the Institution of Civil Engineers – Structures and Buildings* **146(4)**: 381–389.

Pecce M and Fabbrocino G (1999) Plastic rotation capacity of beams in normal and high-performance concrete. *ACI Structural Journal* **96(2)**: 290–296.

Sebastian W and Zhang C (2008) Analysis of concrete structures across the ductility spectrum. *Magazine of Concrete Research* **60(9)**: 685–690.

Sheikh SA and Khoury SS (1993) Confined concrete columns with stubs. *ACI Structural Journal* **90(4)**: 414–431.

Sheikh SA and Yeh CC (1990) Tied concrete columns under axial load and flexure. *Journal of Structural Division, ASCE* **116(10)**: 2780–2801.

Sheikh SA, Shah DV and Khoury SS (1994) Confinement of high-strength concrete columns. *ACI Structural Journal* **91(1)**: 100–111.

Shim CS, Chung YS and Han JH (2008) Cyclic response of concrete-encased composite columns with low steel ratio. *Proceedings of the Institution of Civil Engineers – Structures and Buildings* **161(2)**: 77–89.

Sim JI, Yang KH and Shim HJ (2009) Test on seismic strengthening of RC columns using wire rope and T-plate units. *Magazine of Concrete Research* **61(10)**: 823–836.

Smith RG and Orangun CO (1969) Evaluation of the stress–strain curve of concrete in flexure using method of least squares. *ACI Journal* **66(44)**: 805–822.

SNZ (Standards New Zealand) (2006) NZS 3101: Concrete Structures. Part 1: The design of concrete structures. SNZ, Wellington, New Zealand.

Soliman MTM and Yu CW (1967) The flexural stress–strain relationship of concrete confined by rectangular transverse reinforcement. *Magazine of Concrete Research* **19(61)**: 223–238.

Spence R (2008) Earthquake loss estimation for reinforced concrete buildings: some problems. *Magazine of Concrete Research* **60(9)**: 701–707.

Sturman GM, Shah SP and Winter G (1965) Effects of flexural strain gradients on microcracking and stress–strain behavior of concrete. *ACI Journal* **62(50)**: 805–822.

Supaviriyakit T, Pimanmas A and Warnitchai P (2007) Cyclic response of non-seismically detailed interior RC beam-column connection with varying column tributary area. *Magazine of Concrete Research* **59(5)**: 351–365.

Swartz SE, Nikaeen A, Narayan BHD, Periyakaruppan N and Refai TME (1985) Structural bending properties of high strength concrete. *ACI Special Publication* **87(9)**: 147–178.

Tabsh SW (2006) Elimination of the effect of strain gradient from concrete compressive strength test results. *Computers and Concrete* **3(6)**: 375–388.

Tan TH and Nguyen NB (2004) Determination of stress–strain curves of concrete from flexure tests. *Magazine of Concrete Research* **56(4)**: 243–250.

Tan TH and Nguyen NB (2005) Flexural behavior of confined high-strength concrete columns. *ACI Structural Journal* **102(2)**: 198–205.

Tao Z and Yu Q (2008) Behaviour of CFRP-strengthened slender square RC columns. *Magazine of Concrete Research* **60(7)**: 523–533.

Watson S and Park R (1994) Simulated seismic load tests on reinforced concrete columns. *Journal of Structural Engineering, ASCE* **120(6)**: 1825–1849.

Whitney CS (1940) Plastic theory of reinforced concrete design. *Proceedings of ASCE* **66(10)**: 1749–1780.

Wu YF, Oehlers DJ and Griffith MC (2004) Rational definition of the flexural deformation capacity of RC column sections. *Engineering Structures* **26(5)**: 641–650.

Xiao X, Guan FL and Yan S (2008) Use of ultra-high-strength bars for seismic performance of rectangular high-strength concrete frame columns. *Magazine of Concrete Research* **60(4)**: 253–259.

Yi ST, Kim JHJ and Kim JK (2002) Effect of specimen sizes on ACI rectangular stress block for concrete flexural members. *ACI Structural Journal* **99(5)**: 701–708.

Zhou W and Zheng WZ (2010) Experimental research on plastic design method and moment redistribution in continuous concrete beams prestressed with unbonded tendons. *Magazine of Concrete Research* **62(1)**: 51–64.